1/28-91J50 (1)

UCRL-ID--104993

DE91 006749

Design and Performance of a multiterawatt, Subpicosecond Neodymium Glass Laser

F.G. Patterson and M.D. Perry

September 1990

Lawrence Livermore National Laboratory

This is an informal report intended primarily for internal or limited external distribution. The opinions and conclusions stated are those of the author and may or may not be those of the Laboratory.

Work performed under the auspices of the U.S. Department of Energy by the Lawrence Livermore National Laboratory under Contract W-7405-Eng-48.

MASTER

DISTRIBUTION OF THIS DOCUMENT IS UNLIMITED

DISCLAIMER

This document was prepared as an account of work sponsored by an agency of the United States Government. Neither the United States Government nor the University of California nor any of their employees, makes any warranty, express or implied, or assumes any legal liability or responsibility for the accuracy, completeness, or usefulness of any information, apparatus, product, or process disclosed, or represents that its use would not infringe privately owned rights. Reference herein to any specific commercial products, process, or service by trade name, trademark, manufacturer, or otherwise, does not necessarily constitute or imply its endorsement, recommendation, or favoring by the United States Government or the University of California. The views and opinions of authors expressed herein do not necessarily state or reflect those of the United States Government or the University of California, and shall not be used for advertising or product endorsement purposes.

This report has been reproduced
directly from the best available copy.

Available to DOE and DOE contractors from the
Office of Scientific and Technical Information
P.O. Box 62, Oak Ridge, TN 37831
Prices available from (615) 576-8401, FTS 626-8401.

Available to the public from the
National Technical Information Service
U.S. Department of Commerce
5285 Port Royal Rd.,
Springfield, VA 22161

Price Code	Page Range
A01	Microfiche
Papercopy Prices	
A02	1- 10
A03	11- 50
A04	51- 75
A05	76-100
A06	101-125
A07	126-150
A08	151-175
A09	176-200
A10	201-225
A11	226-250
A12	251-275
A13	276-300
A14	301-325
A15	326-350
A16	351-375
A17	376-400
A18	401-425
A19	426-450
A20	451-475
A21	476-500
A22	501-525
A23	526-550
A24	551-575
A25	576-600
A99	601 & UP

Design and Performance of a Multiterawatt, Subpicosecond Neodymium Glass Laser

F.G. Patterson and M.D. Perry

Laser Program, Lawrence Livermore National Laboratory
MC L-490, Livermore, Ca. 94550

There has been considerable activity recently in the development of small scale, high-power, short-pulse laser systems for applications in multiphoton processes,[1-3] dense plasma physics,[4-6] and XUV lasers.[7,8] To date, the majority of these experiments have been performed with subpicosecond dye[9,10] or excimer[11,12] laser systems. The experiments in multiphoton processes which have been performed with solid-state lasers have generally been performed with longer (>50 psec) pulses.[13,14]

Dye lasers are a natural choice for the generation of subpicosecond pulses due to their large gain bandwidth. Unfortunately, the low saturation fluence and short storage time of dyes limits the available fluence to a few millijoules per square centimeter, severely limiting the peak power attainable from dye laser systems. Excimer based systems exhibit bandwidths capable of supporting pulses as short as 200 fsec and saturation fluences on the order of 10 mJ/cm^2. Although higher than dyes, the low stored energy density of excimers requires the use of large aperture amplifiers to produce pulses exhibiting peak power of more than a few tens of gigawatts. Nevertheless, terawatt scale short-pulse excimer lasers have been demonstrated.[11,12]

Broad-band solid-state materials such as Nd:Glass, Ti:Sapphire and Alexandrite, exhibit saturation fluences on the order of Joules/cm^2. Unfortunately, the large stored energy density of these solid state materials cannot be accessed directly with short pulses due to beam filamentation caused by the intensity dependent refractive index. This limits the power density in a solid-state amplifier to only a few GW/cm^2. The application of chirped-pulse amplification (CPA) to solid-state lasers[15] circumvents this problem. With the CPA technique, a chirped, comparatively long pulse is produced and compressed to a short pulse only after amplification. The intensity in the amplifiers is kept below the level for significant nonlinear phase distortion. In this paper, we present the design and performance of a small scale Nd:Glass laser system employing chirped-pulse amplification to produce subpicosecond pulses exhibiting peak power exceeding 10 TW.

The technique of chirped-pulse amplification (CPA), developed initially for radar, consists of four basic elements: 1) production of a clean, linearly-chirped

pulse of sufficient bandwidth to support the desired final pulse duration, 2) stretching of the pulse to a duration long enough such that the pulse intensity in the amplifiers remains below the limit imposed by nonlinear phase distortion, 3) amplification, 4) compression of the linearly-chirped, amplified pulse to the desired short pulse duration. These elements are realized in our Nd:Glass based laser system as shown in Figs. 1A and 1B.

The laser system begins with a mode-locked Nd:YLF oscillator which produces nearly Gaussian, transform-limited, 50 psec pulses at a 76 MHz repetition rate. A single pulse is selected from the mode-locked train by a dual crystal Pockels Cell. The single pulse is coupled into a ≈400 m single-mode, polarization preserving fused silica fiber by a combination of a 40 cm focal length lens and a 1.2 cm effective focal length diode laser collimating lens. This combination provided a good match to the numerical aperture of the fiber resulting in both good coupling efficiency (60%) and stable fiber alignment. The power into the fiber is controlled by a combination of a half-wave plate and polarizer. An additional half-wave is used just prior to the fiber in order to accurately match the laser polarization to the fiber axis. Due to self-phase modulation (SPM) the pulse exiting a single-mode fiber exhibits a strong power dependent bandwidth below the Raman threshold. Under these conditions, the compressed pulse will exhibit large fluctuations in temporal duration as well as amplitude due to any variations in the pulse energy coupled into the fiber. Variations in the coupled energy can arise from many sources: amplitude or pointing fluctuations in the master oscillator or mechanical-vibrational coupling into the optical components. We are able to minimize these effects in our CPA system by utilizing the results of Heritage et al.[16] These workers demonstrated that a moderately long fiber driven far above the Raman threshold (third Stokes generation) with a mode-locked Nd:YAG pulse can produce large, highly-stabilized spectral regions with a linear chirp (≈60 Å). The highly linear chirp is a consequence of the pulse reshaping which occurs in the fiber as the intense Stokes pulse walks through the pump pulse, preferentially depleting and thus steepening its leading edge.[17] With these very high input powers and steepened leading edge, significant bandwidth is generated early in the fiber, particulary on the red side. Group velocity dispersion (GVD) may thus linearize the chirped red portion of the spectrum even in short fibers (≈145 m)[18] while a longer fiber such as that employed in Reference 16 required to linearize the blue portion of the spectrum since it is primarily produced later in the fiber. Another advantage of operating far above the Raman threshold is that the energy and bandwidth of the pulse exiting the fiber is clamped because any incremental increase in input energy is converted directly into additional energy in the high-order Stokes pulses.[16,18] using the method of spectral windowing[19] as well as streaked spectroscopy, we have verified the results of Reference 16 using the identical fiber with 50 psec Nd:YLF pulses to produce stabilized 500 fsec pulses from a 65 Å linearly-chirped spectrum (Fig. 2A). (The time-bandwidth product for

the square spectrum produced directly out of the fiber is $\Delta\nu \bullet \Delta t = .88$.)

As a result of the combined effects of GVD, SPM and Raman generation the pulse has been broadened and reshaped temporally from the initial 50 psec Gaussian to a pulse of 110 psec duration and a shape similar to that of its spectrum (90 Å bandwidth, Fig. 2A). A reduced spectral region of this chirped pulse will have a correspondingly shorter pulse duration. Due to gain bandwidth narrowing[x] discussed below, only an ≈40 Å spectrum can be maintained in the amplifier system. Therefore, the stretcher used to increase the duration of the chirped pulse prior to amplification has been designed to pass only ≈40 Å, resulting in an initial, effective pulse duration of only about 50 psec. This stretcher, based roughly on the design of Martinez,[20] employs 1200 lines/mm ruled diffraction gratings used near Littrow in a dual pass geometry. Two pairs of lenses (f1=100 cm, f2=10 cm) are used in the stretcher in order to relay the image of the first grating with adjustable magnification. The variable magnification, easily controlled by turning a micrometer to change the position one lens, allows the pulse compression to be quickly and accurately optimized while monitoring the pulse autocorrelation signal. No adjustment of the large, bulky compression gratings is necessary. This unique stretcher and the advantages it offers to CPA-based laser systems is discussed in detail elsewhere.[21] At the focal plane of the stretcher, the frequency components of the chirped pulse are spatially resolved allowing use of a hard filter to eliminate unwanted spectral components.[19] The use of the spectral filter results in a pulse exiting the stretcher having nearly all of its energy linearly chirped. We have used this device to stretch large bandwidth pulses (≈60 Å) from 75 psec to as much as 1.2 nsec. In order to match the 1200 lines/mm compressor used here (≈900 cm grating separation), the stretcher was adjusted to provide 400 psec pulses at an incident bandwidth of 40 Å. Compression of the pulse at this point yields an essentially sinc^2 pulse shape with a time-bandwidth product of $0.95 \pm .06$ in good agreement with model calculations.

The stretched, low energy (1 nJ), p-polarized single pulse is coupled into a ring regenerative amplifier by a 2m single-mode, polarization preserving fiber. The position and focal length of the fiber collimating lens is such that the seed beam is approximately mode-matched into the regenerative amplifier. The ring regenerative amplifier is a stable TEM_{00} laser cavity used to provide a large net gain (10^7) free of spectral modulation.[22] The seed pulse enters the ring regenerative amplifier by passing through a thin-film polarizer (TFP1). The pulse passes through a single crystal Pockels cell, initially with no applied voltage. The pulse exits the Pockels cell on this first pass with its polarization unaltered and hence passes through a second polarizer oriented to reject s-polarized light. The pulse then transits a pair of identical 4x65mm Neodymium doped (3%) HAP3 glass amplifiers. HAP3 is a high thermal conductivity (0.89 W/cm K) phosphate glass exhibiting a peak fluorescence at 1052.6 nm, nearly identical to the central

wavelength of the chirped pulse, 1052.7 nm. The use of this glass type results in symmetric gain narrowing of the chirped pulse spectrum and is important in obtaining high contrast pulses of minimum duration.[23]

The regenerative amplifier can be operated at a variety of repetition rates. When compressed pulses with the best possible contrast ratio are needed a repetition rate of .25 Hz is employed to completely eliminate thermal birefringence which can result in spectral modulation.[x] In this case, the regenerative amplifier is made into a stable resonator by the addition of a single plano-convex lens and the distance around the ring is adjusted to be two focal lengths. If a higher repetition rate is desired (≈2 Hz) the same design is employed except a diverging lens is added to cancel the thermal focussing in the Nd:glass laser rods. The dual amplifier arrangement employed here, minimizes the unavoidable effects of thermal birefringence.[24] A 90 degree rotator placed after the first amplifier not only rotates the average polarization of the beam from p to s but also rotates the polarization ellipse of those areas of the beam which have become depolarized. Passage through a second identical amplifier then (partially) cancels the birefringent depolarization introduced by the first. The pulse next passes through a hard aperture. The aperture serves an important function in discriminating against amplified spontaneous emission and defining the cavity mode. Only the radiation emitted in the cavity mode defined by the limiting aperture can be amplified. The long optical path length around the cavity (3 m) increases the ability of the resonator discriminate against the ASE and also reduces the rise time requirements on the high voltage pulse which drives the Pockels cell.

After reflection by three cavity mirrors, the now s-polarized pulse is incident upon TFP1 at Brewster's angle and is reflected with nearly 100% efficiency by this polarizer. Shortly after the pulse made its initial pass through the Pockels cell, a fast high voltage pulse was applied to the KD*P Pockels cell to provide a half-wave retardation. The voltage pulse has a risetime of ≈1 nsec and is derived from a planar triode driver. A splitter/inverter is used to place +4 kV on one side of the Pockels cell and -4 kV on the other yielding a net 8 KV applied to the Pockels cell. The pulse, rotated to p-polarization by the Pockels cell, passes the second polarizer and begins another trip around the cavity. The Pockels cell remains biased at the half-wave voltage, trapping the pulse in the regenerative amplifier for the desired number of passes through the gain medium. The pulse is ejected from the cavity by dropping the Pockels cell voltage to ground. This causes an s-polarized pulse to strike TFP2, resulting in its reflection out of the cavity.

After the regenerative amplifier, the 10 mJ pulse is propagated through a relay-imaged, B-integral-limited amplifier chain (Fig. 1B). The design of this optical system is patterned after that employed by the world's most powerful laser, the Nova fusion laser located at Lawrence Livermore National Laboratory.[25] After expansion to ≈8 mm ($1/e^2$), the Gaussian (spatial) laser beam illuminates an

≈2.5 mm serrated aperture[26]. The image of this aperture is relayed by a series of spatial filters down the amplifier chain. There are three advantages to this technique. First, the image of this aperture gives a nearly uniform (square) beam profile, resulting in a 1:1 peak to average ratio (ideal case). In contrast, a Gaussian beam profile has a 2:1 peak to average ratio. Thus for a given amplifier aperture size, a uniform beam profile allows a larger pulse energy to be extracted while maintaining a lower peak intensity. Second, the steep rising edge of the uniform beam profile allows a larger fill factor to be used in the amplifiers compared to Gaussian beams which are usually employed. The Gaussian beam fills only ≈22% of the volume of a laser rod with diameter d=3w, whereas an approximately uniform beam profile fills ≈86% of the rod volume at the same diameter.[27] Third, the impact of diffraction effects from the phase and amplitude aberrations which are always present even in high quality optical components is minimized because the amplifier heads and other damage prone optical elements (e.g., Faraday rotators) are positioned as closely as possible to the aperture image planes, i.e., in the near field where ripple growth due to diffraction has not had the opportunity to develop.[25]

The energy and optical parameters for propagation through the amplifier chain is as follows (see Figs. 1A and 1B). The 1 mj pulse which transmits the serrated aperture is relayed with an air spatial filter (ASF, f#=61, M=2.3) through two LG-760 Nd:Phosphate glass amplifier rods of 9 mm diameter. Next, the 100 mj output pulse is relayed by a vacuum spatial filter (VSF1, f#=17.4, M=3) through a 30 mm diameter permanent magnet Faraday rotator and a 19 mm diameter rod amplifier consisting of HAP3 laser glass. The 1.5 J output from this amplifier is relayed into the final 45 mm rod amplifier with a VSF2 of f#=8.7 and M=2.3. A pulsed magnet Faraday rotator with a diameter of 80 mm is used to isolate the 45 mm amplifier from the rest of the amplifier chain. The final 11 J pulse is relayed into the compressor system with VSF3 (f#=20, M=2.5).

Relay imaging (with magnification) into the pulse compressor is important for two reasons. The beam is expanded to a 10 cm diameter in order to keep the fluence below the damage threshold of the gratings. The highest fluence occurs on the first of our three grating compressor. The three grating design is a simple modification of the conventional double-pass dual grating compressor with the third grating vertically displaced above the first. This is necessary to fit a full 10 cm diameter beam in a double-pass geometry using our 1200 lines/mm, 154 x 200 mm, ruled gratings. The beam encounters the first grating at 35 degrees, slightly off Littrow (39.2°) and is dispersed over a ≈9 m slant distance to the second grating. The beam is retroreflected upward at a slight angle (≈2°) in order to be vertically displaced 30 cm upon completion of the second pass. Compression is stopped at this point by a third grating which diffracts (and collimates) the beam to a final mirror for passage to the target chamber. The fluence on the first grating is less than 100 mJ/cm^2. This is nearly a factor of four below the damage threshold measured by others for these gratings.[28]

The second reason for beam expansion is to keep the peak power below the level at which nonlinear effects become important both for propagation in air and transmission through optics (e.g. vacuum windows, conversion crystals, lenses). The most significant of these is wavefront distortion of the beam arising from the nonlinear refractive index, n_{2I}. This distortion can lead to self-focusing/filamentation of high-power beams. The degree of phase distortion induced by nonlinear propagation is quantified by calculating the "B-Integral,[29]

$$B = \frac{2\pi}{\lambda} \cdot \int_0^L n_{2I}(z) \cdot I(z)\ dz \qquad (1)$$

where I(z) is the intensity as a function of position, L is the pathlength through the optical element under consideration and λ is the laser wavelength. Values of B should be kept as low as possible and should never be greater than approximately π in order to maintain near diffraction limited beam quality and avoid the self-focusing problems mentioned previously. For the 1 cm thick fused silica windows used in our system, $n_{2I}=3\cdot10^{-16}$ cm^2/W, a 10 TW beam with a diameter of 10 cm results in a B value of 2.3, below the value required for significant degradation of beam quality.

Beam quality is monitored on a shot to shot basis by an imaging system coupled to a CCD camera. The beam exiting the vacuum spatial filter and viewed after all transmitting optics is a near diffraction-limited. However, a double-pass through the compressor imparts a periodic modulation on the wavefront which degrades the beam quality. This problem has been traced to a defect in the manufacturing process of the gratings which has recently been corrected. Tests of small sample gratings produced by an interferometrically-controlled ruling process show no detectable degradation of beam quality. New large area gratings are currently being manufactured.

Most Nd:Phosphate glasses exhibit a fluorescence linewidth greater than 20 nm. However, the frequency dependence of the gain coefficient results in distortion and exponential narrowing of the spectrum of an initially broad band pulse subjected to strong amplification. Specifically, the spectral distribution exiting a multipass amplifier, $I_{out}(\omega)$, is related to the input spectrum, $I_{in}(\omega)$, by

$$I_{out}(\omega) = I_{in}(\omega) \cdot [1-\beta(\omega)]^N \cdot G_0(\omega)^N \qquad (2)$$

where $\beta(\omega)$ is the per pass loss, $G_0(\omega)$ is the frequency-dependent small signal gain and N is the number of passes. This expression is strictly valid only in the small-signal limit. Saturation effects will tend to distort the spectrum of a chirped-pulse[30] and can compromise the quality of the chirped-pulse. These effects are negligible

in the system described here since the fluence in the amplifier chain never rises above one-third of the saturation fluence. Hence, equation (2) is adequate to describe the effect of amplification on the spectrum of the chirped input pulse. In the case of frequency independent loss, the spectral narrowing is determined solely by the total gain, $G_0(\omega)^N$.

In order to obtain the shortest compressed pulse, it is necessary to minimize the degree of gain narrowing while simultaneously shaping the chirped spectrum.[23] The simple equation above suggests three methods to maximize the spectral width of an amplified pulse: 1) decrease the system losses to minimize the total gain required to attain the necessary energy output. 2) Broaden the gain profile, $G_o(\omega)$. 3) include a frequency dependent loss, $\beta(\omega)$, which reduces the net gain at the peak of the gain profile. In the system described here, the degree of gain narrowing is carefully controlled to shape and optimize the spectrum to generate high-contrast, transform-limited compressed pulses with a minimum time-bandwidth product. This requires an effective gain profile which is nearly Gaussian near the peak and is incompatible with method (3) described above. The first two methods of reducing gain narrowing are employed as described below.

Our system is designed to amplify a chirped, 1 nJ pulse to a final energy >10 J, a net gain of $\approx 1\times10^{10}$. The majority of this occurs in the regenerative amplifier where the 1nJ pulse is amplified to 10 mJ. For this reason, our efforts to control gain narrowing are concentrated here. After many experiments in which several different regenerative amplifier designs were examined, the ring regenerative amplifier (described in more detail elsewhere[x]) was chosen as that providing the highest gain per pass while maintaining the minimum frequency independent loss. This regenerative amplifier provides a net gain of approximately 1×10^7 (from ~ 1 nJ to 10 mJ) for only 10 round-trips corresponding to a net single-pass gain of five. The round-trip losses are close to 20% resulting in a total gain of 8×10^7. The remaining amplifiers provide gains of 10, 10, 15, and 7.3, respectively for a total system gain of approximately 8.8×10^{11} and a corresponding net gain of 1×10^{10}. For an 11 Joule pulse exiting the amplifier chain 7.5 J are obtained out of the compressor, corresponding to a grating efficiency of 91%. The output spectra and autocorrelation of the compressed pulse are shown in Fig. 2 along with the corresponding calculated results. The measured time-bandwidth product of $0.48\pm.06$ agrees well with the calculated values (.51).

The calculations presented in Figs. 2 are the results of a six-step model of our system: 1) the electric field, $E(\omega)$, exiting the fiber is calculated from the Fourier transform of a linearly-chirped, smoothed square pulse, 2) the pulse stretcher is represented by a quadratic phase factor, 3) any spectral filtering is taken as amplitude modulation, 4) amplification with the detailed frequency-dependent gain profile exhibited by the particular Nd:Phosphate glass chosen, 5) compression is

represented by the quadratic part of the phase factor (a linear compressor) of the double-pass grating pair, 6) the temporal distribution is then calculated by the inverse Fourier transform of the compressed pulse. The approximation of the grating stretcher/compressor as contributing a purely quadratic phase (linear compressor) is quite accurate for the bandwidth and compression factor considered here.

In conclusion, we have developed a Nd:phosphate Glass laser system capable of producing 7.5 Joules in 700 fsec (10.7 TW) with a uniform beam spatial profile. The pulse repetition rate is one shot every four minutes.

Acknowledgements

We would like to thank R. Olsen and J. Weston of Continuum for there help with amplifier components. We would also like to thank E. Prochnow of LLNL and J. Linke of Applied Optics for cutting and polishing the laser rods and G. Edwards for sol-gel coating. Particular thanks to R. Gonzales and K. Haney for technical support and E.M. Campbell for helpful discussions and encouragement. This work was performed under the auspices of the U.S. Department of Energy by Lawrence Livermore National Laboratory under contract # W-7405-Eng-48.

References

1. U.Johann, etc
2. M.D. Perry, A.Szoke, O.L. Landen, and E.M. Campbell, "Nonresonant Multiphoton Ionization: Theory and Experiment," Phys. Rev. Lett., (1988).
3. R.R. Freeman, P.H. Bucksbaum, H. Milchberg, S. Darack, D. Schumacher, and M.E. Geusic,"Above-Threshold Ionization with subpicosecond laser pulses," Phys. Rev. Lett. **59**, 1092 (1987).
4. H. Milchberg,
5. M.M. Murnane, H.C. Kapteyn, and R.W. Falcone, "High-density plasmas produced by ultrafast laser pulses," Phys. Rev. Lett.,**62**, 155 (1989).
6. O.L. Landen, Phys. Rev. Lett., (1989)
7. N.H. Burnett and P.B. Corkum, J. Opt. Soc. Amer. B, (1989); M.D. Perry an C.Keane, "Ultrahigh Brightness Lasers and their Applications," ET&R (1988).
9. M.D. Perry, O.L. Landen, J. Weston, and R. Ettlebrick, Opt. Lett.,
10. M.M. Murnane, and R.W. Falcone, J. Opt. Soc. Amer. B, **5**, 1573 (1988).
11. T.S. Luk, A.McPherson, G. Gibson, K. Boyer, and C.K. Rhodes, Opt. Lett., **14**, 1113.
12 S. Watanabe, A.Endoh, M. Watanabe, N.Sarukura, and K. Hata, J. Opt.

Soc. Amer. B, **6** 1870 (1989).
13. A.L'Hullier,
14. A. L'Hullier, "Harmonic Generation at high laser intensity," Phys. Rev. A, (1989)
15. D. Strickland and G. Mourou, Opt. Comm. **56**, 219 (1985); P. Maine, D. Strickland, P.Bado, M. Pessot, and G. Mourou, IEEE J. Quantum Electron. **24**, 398 (1988).
16. J.P. Heritage, A.M. Weiner, R.J. Hawkins and O.E. Martinez, Opt. Comm. **67**, 367 (1988).
17. R.H. Stolen and A.M. Johnson, IEEE J. Quantum Electron. **QE-22**, 2154 (1986).
18. A.M. Weiner, J.P. Heritage and R.H. Stolen, J. Opt. Soc. Am. **B5**, 364 (1988).
19. J.P. Heritage, R.N. Thurston, W.J. Tomlinson, A.M. Weiner and R.H. Stolen, Appl. Phys. Lett. **47**, 87 (1985); R.N. Thurston, J.P. Heritage, A.M. Weiner, and W.J. Tomlinson, IEEE J. Quantum Electron. **22**, 682 (1986).
20. O.E. Martinez, IEEE J. Quantum Electron. **Qe-23**, 59 (1987).
21. F.G. Patterson, "Continuously Adjustable Laser Pulse Stretcher with Magnification", to be published.
22. M.D. Perry and F.G. Patterson, "A Ring Regenerative Amplifier for Chirped Pulse Amplification Systems", to be published.
23. M.D. Perry, F.G. Patterson, and J. Weston, Opt. Lett., **15**, 381 (1990).
24. W. Koechner, Solid-State Laser Engineering, (Springer-Verlag,1976).
25. J.T. Hunt, P.A. Renard and W.W. Simmons, Appl. Opt. **16**, 779 (1977).
26. serrated aperture
27. A.E. Siegman, Lasers, (University Science Books,1986).
28. Japanese Ref. for grating damage level.
29. D.C. Brown, The Physics of High Peak Power Nd:Glass Laser Systems (Springer-Verlag,1980).
30. J.D. Kafka and J.B. Clark, Ultrafast Phenomena VI, p.30, (Springer-Verlag, 1988).

Figure Captions

1. A) Layout of the front end of the CPA laser system, ASF= air spatial filter, TFP= thin film polarizer. B) Large amplifier and compression section of the CPA system, VSF=vacuum spatial filter.

2. A) Chirped Spectrum with a 2 watt output from the 400 m fiber. B) Measured and calculated amplified spectra at the 10 mj level out of the ring regenerative amplifier. A total gain of 8×10^7 is assumed for the calculated spectrum. C) Measured and calculated autocorrelation signals for the spectrum of Fig. 2A. The agreement between the measured and calculated time-bandwidth products is excellent, indicating that the amplified, compressed pulse are very close to Fourier transform-limited.

Figure 1A

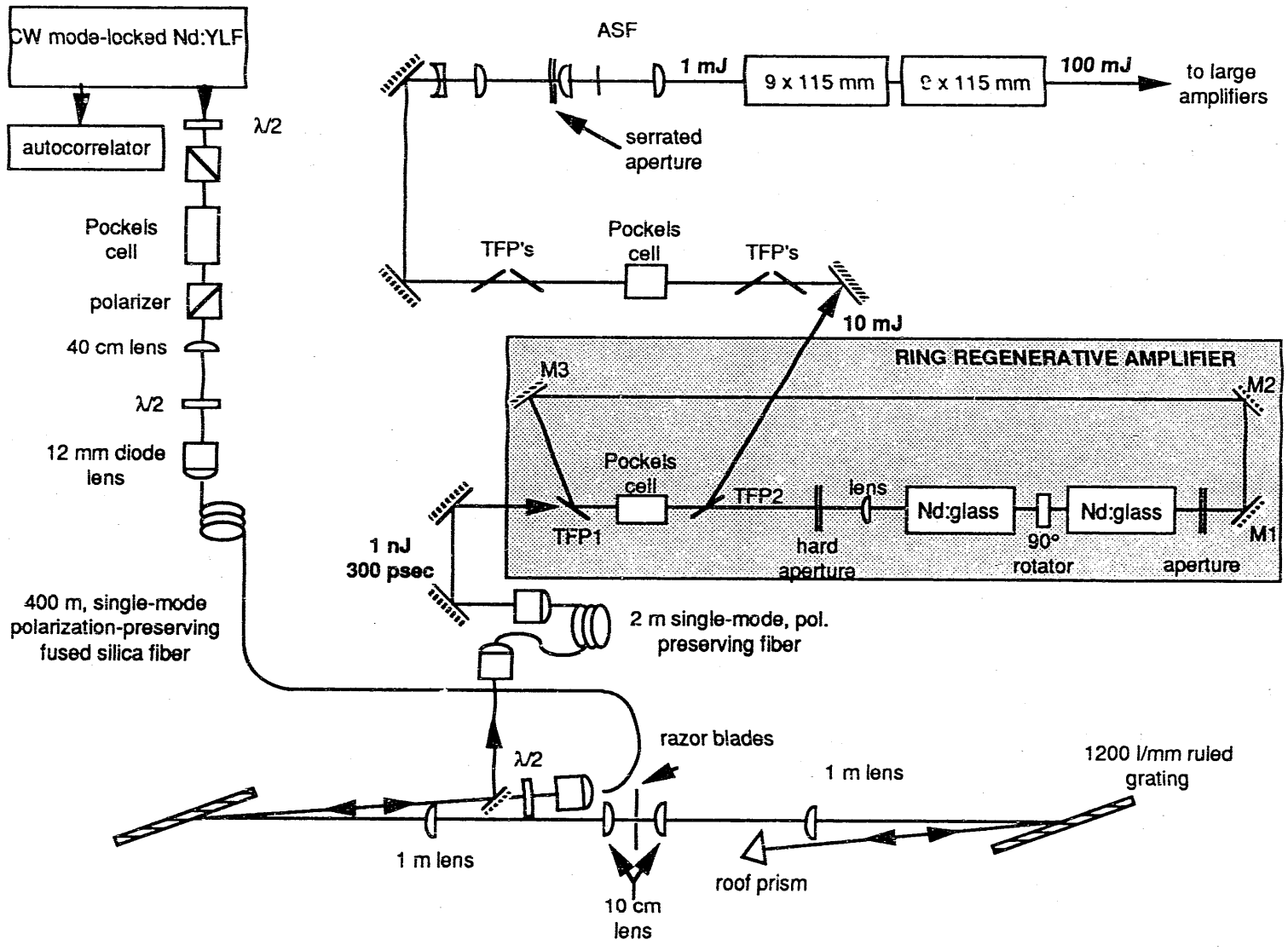
CW mode-locked Nd:YLF
autocorrelator
λ/2
Pockels cell
polarizer
40 cm lens
λ/2
12 mm diode lens
400 m, single-mode polarization-preserving fused silica fiber
ASF
1 mJ
9 x 115 mm
9 x 115 mm
100 mJ
to large amplifiers
serrated aperture
TFP's
Pockels cell
TFP's
10 mJ
RING REGENERATIVE AMPLIFIER
M3
M2
Pockels cell
TFP1
TFP2
hard aperture
lens
Nd:glass
90° rotator
Nd:glass
aperture
M1
1 nJ
300 psec
2 m single-mode, pol. preserving fiber
razor blades
λ/2
1 m lens
1 m lens
10 cm lens
roof prism
1200 l/mm ruled grating

Figure 1B

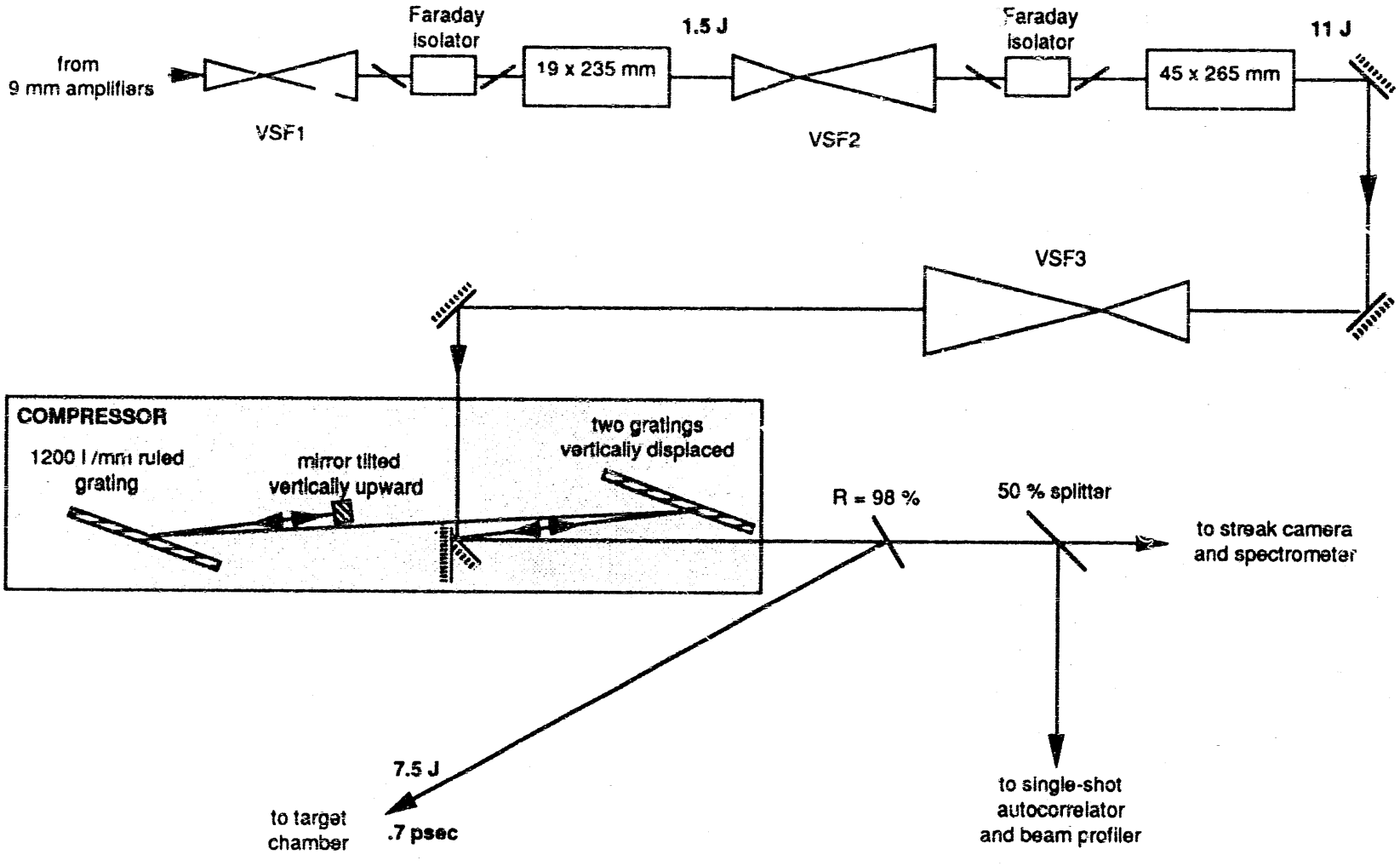
from
9 mm amplifiers
VSF1
Faraday
isolator
19 x 235 mm
1.5 J
VSF2
Faraday
isolator
45 x 265 mm
11 J
VSF3
COMPRESSOR
1200 l /mm ruled
grating
mirror tilted
vertically upward
two gratings
vertically displaced
R = 98 %
50 % splitter
to streak camera
and spectrometer
7.5 J
.7 psec
to target
chamber
to single-shot
autocorrelator
and beam profiler

Figure 2

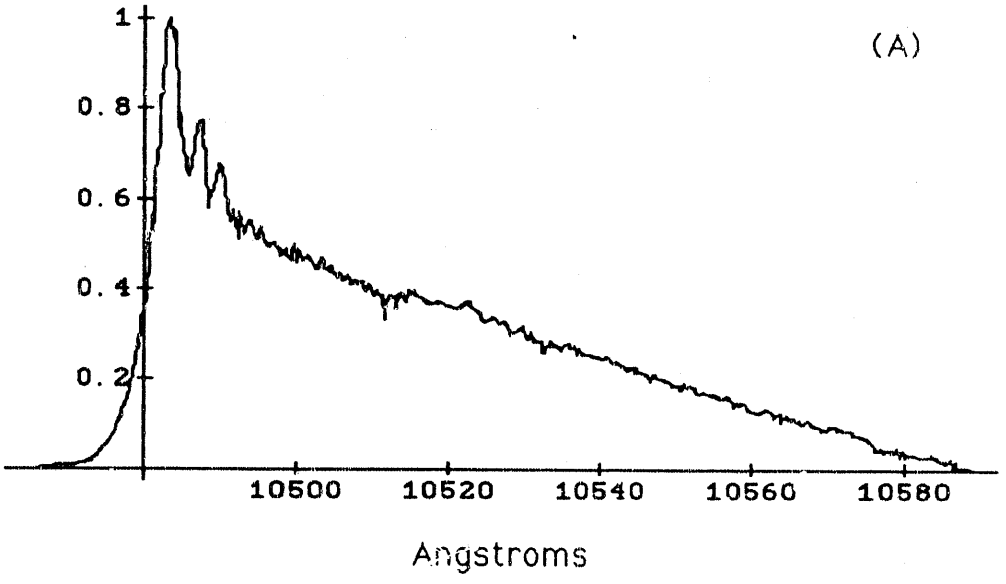
(A)
1
0.8
0.6
0.4
0.2
10500
10520
10540
10560
10580
Angstroms

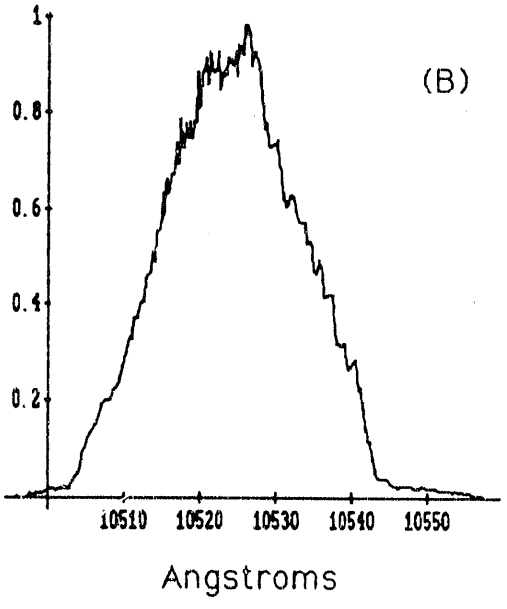
(B)
1
0.8
0.6
0.4
0.2
10510
10520
10530
10540
10550
Angstroms

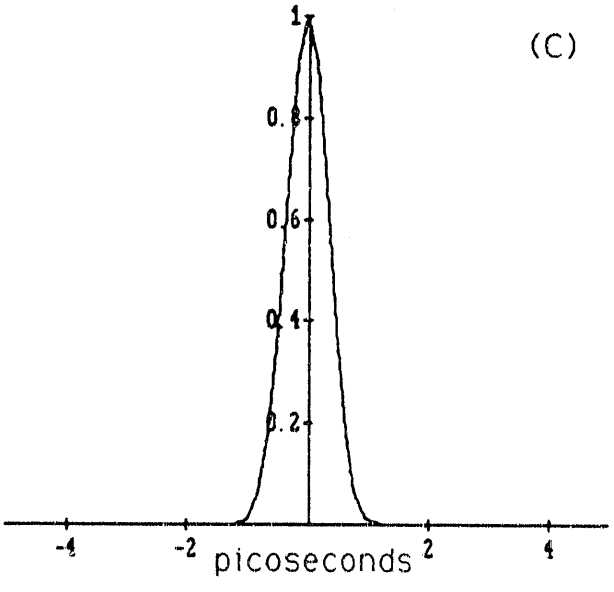
(C)
1
0.8
0.6
0.4
0.2
-4
-2
picoseconds
2
4

END

DATE FILMED

02 / 06 / 91